Electronic Supplementary Material (ESI) for Nanoscale Horizons.

ELECTRONIC SUPPLEMENTARY INFORMATION (ESI)

Size-dependent diffusion of supported metal nanoclusters: Mean-field-type treatments and beyond for faceted clusters

King C. Lai,[1,2,#] Charles T. Campbell,[3] and James W. Evans[1,2,*]

[1]Divison of Chemical & Biological Sciences, Ames National Laboratory - USDOE, Ames, Iowa 50011
[2]Department of Physics & Astronomy, Iowa State University, Ames, Iowa 50011
[3]Chemistry Department, University of Washington, Seattle, Washington 98195

[#]Current address: Fritz Haber Institut der Max Planck Gesellschaft, 14195 Berlin Germany
*Email: evans@ameslab.gov

S1. Refined Gibbs-Thompson type formulation for small faceted nanoclusters

The standard Gibbs-Thompson (GT) treatment of the energetics and chemical potential for nanoclusters (NCs) of size N atoms writes the system energy, E_N, or free energy as the sum of a bulk term, $\mu_\infty N$, and an interface or surface term, $\Gamma N^{2/3}$ (scaling like NC surface area). This leads to a standard GT-type expression for the chemical potential, $\mu_N = dE_N/dN = \mu_\infty + (2\Gamma/3) N^{-1/3}$ (noting that $N^{1/3}$ is proportional to R, an effective radius of curvature for the 3D NC [1,2]). This formulation can be applied to either unsupported or supported NCs. However, for small faceted NCs the above formulation is not expected to be effective, and instead it is more natural to write

$E_N = \mu_\infty N$ (bulk) + $\Gamma_1 N^{2/3}$ (surface) + $\Gamma_2 N^{1/3}$ (edge) + $\Gamma_0 N^0$ (vertex), so (s1)

$\mu_N = dE_N/dN = \mu_\infty + (2\Gamma_1/3) N^{-1/3} + (\Gamma_2/3) N^{-2/3}$. (s2)

This formulation has been used previously to fit the energetics for supported TPs [3].

For another perspective on behavior for {100}-epitaxially supported faceted NCs, it is instructive to consider behavior for the sequence of "ideal" closed-shell TPs described in the main text. These have an equal number of atoms along the edge between adjacent {111} side facets, and along the edges between the {100} top and {111} side facets. Consequently, they mimic the continuum Winterbottom shape for the NC for our lattice-gas model. These correspond to sizes N = 13, 50, 126,… for heights k = 2, 3, 4,… In general, for these ideal closed-shell TPs, one has that

$N = N(k) = k(2k-1)(7k-1)/6 = (14k^3 - 9k^2 + 1)/6$ (s3)

and $E_N = E_{N(k)} = -(14k^3 - 16k^2 + 6k - 1)\phi$. (s4)

Thus, for large k (and N), it is clear that $E_N \approx -6\phi\, N$, yielding a limiting value for the chemical potential, $\mu_\infty = dE_N/dN \approx -6\phi$. This result reflects the feature that each atom in the bulk of an fcc crystal has 12 shared bonds to neighboring atoms.

Introducing a new variable $y = (6N/14)^{1/3}$, it is convenient to rewrite (s3) as

$$y = k[1 - (9/14)k^{-1} + (1/14)k^{-2}]^{1/3} \quad \text{or} \quad y^{-1} = k^{-1}\,[1 - (9/14)k^{-1} + (1/14)k^{-2}]^{-1/3}. \qquad \text{(s5)}$$

Rewriting the second expression as a Taylor expansion for y^{-1} in terms of k^{-1} yields

$$y^{-1} = k^{-1}\,[1 + (3/14)k^{-1} + (10/147)k^{-2} + (5/196)k^{-3} + (515/49392)k^{-4} + \ldots]. \qquad \text{(s6)}$$

Inversion of this series then yields

$$k^{-1} = y^{-1}\,[1 - (3/14)y^{-1} + (1/42)y^{-2} - (5/2744)y^{-3} + (61/345744)y^{-4} + \ldots], \text{ so} \qquad \text{(s7)}$$

$$k = y[1 - (3/14)y^{-1} + \ldots]^{-1} = y[1 + (3/14)y^{-1} + (13/588)y^{-2} + (1/686)y^{-3} + \ldots]. \qquad \text{(s8)}$$

Finally, substituting (s8) into (s4) yields

$E_N =$

$$-14y^3\,\{[1+(3/14)y^{-1}+\ldots]^3 - (8/7)y^{-1}[1+(3/14)y^{-1}+\ldots]^2 + (3/7)y^{-2}[1+(3/14)y^{-1}+\ldots] - (1/14)y^{-3}\}\,\phi$$

$$= -14y^3\,\{1 - (1/2)y^{-1} + (1/7)y^{-2} - (47/1176)y^{-3} + (647/403368)y^{-4} - \ldots\}\,\phi$$

$$= -6\phi\, N\,\{1 - (1/2)(3/7)^{-1/3}\, N^{-1/3} + (1/7)(3/7)^{-2/3}\, N^{-2/3} - (47/1176)(3/7)^{-1}\, N^{-1} + \ldots\}. \qquad \text{(s9)}$$

Consequently, for large N, one has that

$$\mu_N = dE_N/dN = \mu_\infty\,\{1 - (1/3)(3/7)^{-1/3}\, N^{-1/3} + (1/21)(3/7)^{-2/3}\, N^{-2/3} - \ldots\}, \qquad \text{(s10)}$$

i.e., a Taylor series expansion for μ_N in powers of $N^{-1/3}$.

In summary, as anticipated by the heuristic expression (s2), the chemical potential of atoms in small faceted NCs is not well-described by a standard GT type relation, $\mu_N = \mu_\infty + (2\Gamma/3)R^{-1}$, associated with bulk and surface contributions to the NC energy. Here, $R = N^{1/3}$ is an effective NC radius of curvature. Rather, it is more appropriate to include additional terms reflecting edge and vertex contributions to the NC energy. The edge contribution to the chemical potential is expected to scale like R^{-2}. However, utilizing an exact expression for the energy of "ideal" truncated pyramids in our atomistic lattice-gas model, we find that the chemical potential as calculated via $\mu_N = dE_N/dN$ is given by an inverse power series in $N^{1/3}$ or R, (s10). Calorimetric evidence for the need for such corrections to GT-type relations has been presented [4].

S2. Comprehensive analysis of the size-dependent NC thermodynamics

Table S1 provides an expanded version of Table I where thermodynamic and structural information is provided for the ground state NC configurations in our stochastic lattice-gas model for sizes N = 13 - 126.

Table S1. Comprehensive analysis of ground state configurations and energetics for the lattice-gas model for {100} epitaxially supported 3D clusters sizes N = 13-126 with f = 0.75. Particularly stable closed-shell NC sizes are indicated in larger bold red font. Note that these display strong local minima in D_N. Other less stable closed shell-sizes are indicated in smaller non-bold red font. We also indicate other NC sizes where D_N has local maxima and local minima. We also indicate in green font cases where a few atoms are added to a closed-shell size, NC_s, but the base is actually smaller than for N_{cs} due to substantial rearrangement of the NC configuration.

N	N_{base}	k	-E/ϕ	-ΔE/ϕ	D_{700K}
13	**3x3=9**	**2**	**59**	**6**	**min**
14	9,10	2,3	63	4	max
15	11	2	68	5	
16	11,12	2	72	5	
17	12	2	78	5	
18	**3x4=12**	**2**	**84**	**6**	**min**
19	12,13	2,3	88	4	
20	12,14	2,3	93	5	max
21	14,15	2	98	5	
22	15,16	2	103	5	
23	15	2	109	6	
24	16	2	114	5	
25	**4x4=16**	**2**	**120**	**6**	**min**
26	16,17	2,3	124	4	
27	16,18	2,3	129	5	max
28	16,18,19	2,3	134	5	
29	4x4=16	3	140	6	
30	19	2	145	5	
31	20	2	150	5	
32	**4x5=20**	**2**	**156**	**6**	**min**
33	20,21	2,3	160	4	
34	19,20,22	2,3	165	5	max
35	20,22,23	2,3	170	5	
36	20	3	176	6	
37	20,23	2,3	181	5	
38	4x5=20	3	187	6	min
39	24	2	192	5	~min
40	25	2	197	5	
41	**5x5=25**	**2**	**203**	**6**	**~min**
42	25,26	2,3	207	4	
43	25,27	2,3	212	5	
44	25,27,28	2,3	217	5	
45	24,25	3	223	6	
46	24,25,28	2,3	228	5	
47	24,25	3	234	6	
48	25,29	2,3	239	5	
49	25	3	245	6	
50	**5x5=25**	**3**	**251**	**6**	**min**

N	N_{base}	k	-E/ϕ	-ΔE/ϕ	D_{700K}
50	**5x5=25**	**3**	**251**	**6**	**min**
51	25,26	3,4	255	4	
52	25,27	3,4	260	5	
53	25,27,28	3,4	265	5	max
54	5x5=25	4	271	6	
55	28	3	276	5	
56	29	3	281	5	
57	29	3	287	6	
58	30	3	292	5	
59	30	3	298	6	
60	30	3	303	5	
61	30	3	309	6	~min
62	**5x6=30**	**3**	**315**	**6**	**min**
63	30,31	3,4	319	4	
64	30,32	3,4	324	5	
65	30,32,33	3,4	329	5	max
66	30	4	335	6	
67	30,33	3,4	340	5	
68	5x6=30	4	346	6	
69	34	3	351	5	
70	34,35	3	356	5	
71	35	3	362	6	
72	35,36	3	367	5	
73	35,36	3	373	6	
74	35	3	379	6	min
75	36	3	384	5	~min
76	36	3	390	6	~min
77	**6x6=36**	**3**	**396**	**6**	**~min**
78	36,37	3,4	400	4	
79	36,38	3,4	405	5	
80	36,38,39	3,4	410	5	max
81	36	4	416	6	
82	36,39	3,4	421	5	
83	36	4	427	6	
84	36,40	3,4	432	5	
85	36	4	438	6	
86	6x6=36	4	444	6	~min

N	N_{base}	k	-E/ϕ	-ΔE/ϕ	D_{700K}
86	6x6=36	4	444	6	~min
87	36,37,41,42	3,4,5	448	4	
88	41,42	3	454	6	~min
89	41	3	460	6	~min
90	42	3	465	5	~min
91	42	3	471	6	~min
92	**6x7=42**	**3**	**477**	**6**	**min**
93	42,43	3,4	481	4	
94	42,44	3,4	486	5	
95	41,42,44,45	3,4	491	5	max
96	42	4	497	6	
97	42,45	3,4	502	5	
98	42	4	508	6	
99	42,46	3,4	513	5	
100	41	4	519	6	
101	42	4	525	6	
102	42	4	530	5	
103	42	4	536	6	min
104	6x7=42	4	542	6	~min
105	42,43	4,5	546	4	
106	48	3	552	6	
107	48	3	558	6	min
108	48,49	3,4	563	5	~min
109	49	3	569	6	~min
110	**7x7=49**	**3**	**575**	**6**	**~min**
111	48,49,50	3,4	579	4	
112	49,51	3,4	584	5	max
113	46,49,51,52	3,4	589	5	~max
114	49	4	595	6	
115	49,52	3,4	600	5	
116	49	4	606	6	
117	49,53	3,4	611	5	
118	48	4	617	6	
119	49	4	623	6	
120	49	4	628	5	
121	49	4	634	6	
122	49	4	640	6	min
123	49	4	645	5	
124	49	4	651	6	
125	49	4	657	6	~min
126	**7x7=49**	**4**	**663**	**6**	

S3. Schematics for interlayer diffusion and corner rounding at the NC base

Figure S1 provides a schematic illustrating the interlayer diffusion process in our stochastic model. This process follows the default prescription for the model of hopping to available NN fcc sites which are connected to the NC. Specifically, for all types of close-packed monoatomic steps, downward interlayer transport involves a first lateral hop which positions the atom partly overhanging the step edge followed by a second downward hop to an fcc adsorption site at the base of the step.

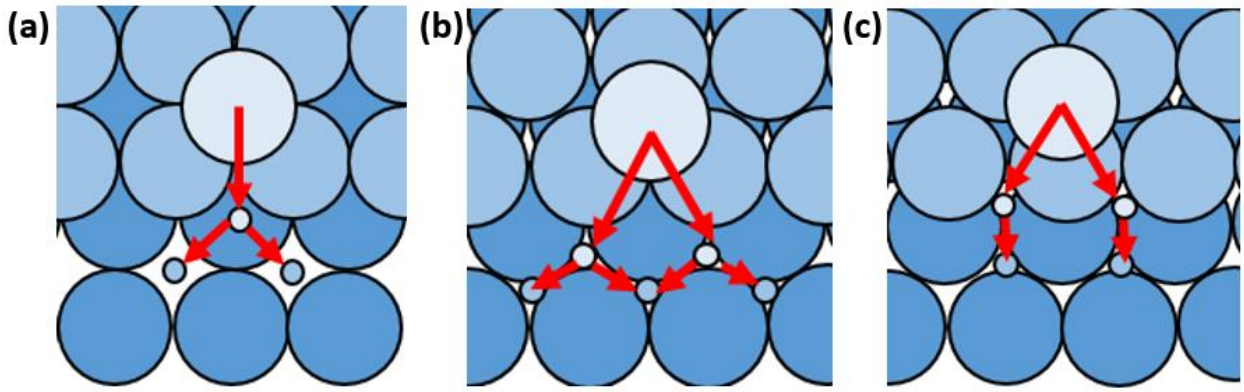

Figure S1. Downward interlayer transport at close-packed steps in our stochastic model via a sequence of two hops to NN fcc sites: (a) {111}-microfaceted step on a stepped {100} surface; (b) {111}-microfaceted step and (c) {100}-microfaceted step on a stepped {111} surface.

Figure S2 provides a schematic illustrating corner rounding in our stochastic model of a hopping atom at the rectangular based of a supported NC. This process involves hopping to a second NN site where the atom is disconnected from (i.e., not bonded to atoms in) the NC. However, the atom remains four-fold coordinated to the substrate.

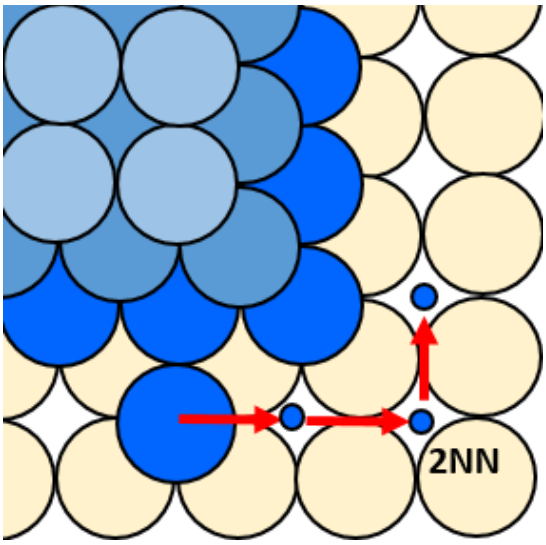

Figure S2. Corner rounding of an atom via a 2NN site at the rectangular base of a NC. Substrate atoms are shown in yellow and NC atoms in various shades of blue.

S4. CM motion of NCs induced by surface atom hops

For atoms hopping "horizontally" on the top {100} facet, or along the base of the NC, it is clear that each hop of distance 'a' (the surface lattice constant) of the atom to a NN site produces a lateral shift in the NC center of mass (CM) position of $\delta R_{CM} = a/N$.

However, for atoms hopping on the sloped {111} side facets, the situation is more complicated. See **Figure S3**. Of the 6 possible hops between fcc(111) adsorption sites on the side facet, two are "horizontal" of distance 'a' as for hops on the top {100} facets and along the base. Consequently, these also produce a lateral shift in the NC CM of $\delta R_{CM} = a/N$. In contrast, for the other 4 possible hops, the horizontal projection of the atom motion only corresponds to a distance $2^{-1/2}$ a, so the lateral shift of the CM is $\delta R_{CM} = 2^{-1/2}\, a/N$.

Considering the random walk of the atom on a (large) {111} side facet, if $\mathbf{r}_j$ denotes the horizontal projection of the displacement on the j^{th} hop, then the horizontal displacement of the CM of the NC after n atop hops is given by $\delta \boldsymbol{R}_n = \sum_{j=1-n} \mathbf{r}_j/N$. Given that $\mathbf{r}_j$ are independent for different j, but have the same probability distribution satisfying $\langle \mathbf{r}_j \rangle = \mathbf{0}$ for each j, from the above analysis it follows that

$$\langle \mathbf{r}_i.\mathbf{r}_j \rangle = 0 \text{ for } i \neq j, \text{ and } \langle \mathbf{r}_j.\mathbf{r}_j \rangle = 4/6\ (2^{-1/2}a)^2 + 2/6\ (a)^2 = (2/3)a^2. \quad \text{(s11)}$$

It then follows that

$$\langle \delta \boldsymbol{R}_n \cdot \delta \boldsymbol{R}_n \rangle = \sum_{j=1-n} \langle \mathbf{r}_j.\mathbf{r}_j \rangle / N^2 = n \langle \mathbf{r}_j.\mathbf{r}_j \rangle / N^2 = n\ (2/3)a^2/N^2. \quad \text{(s12)}$$

This result leads to the additional factor of 2/3 appearing in the expression (4) for $D_N(111)$ relative to the expressions (3) for $D_N(100)$ and $D_N(\text{base})$.

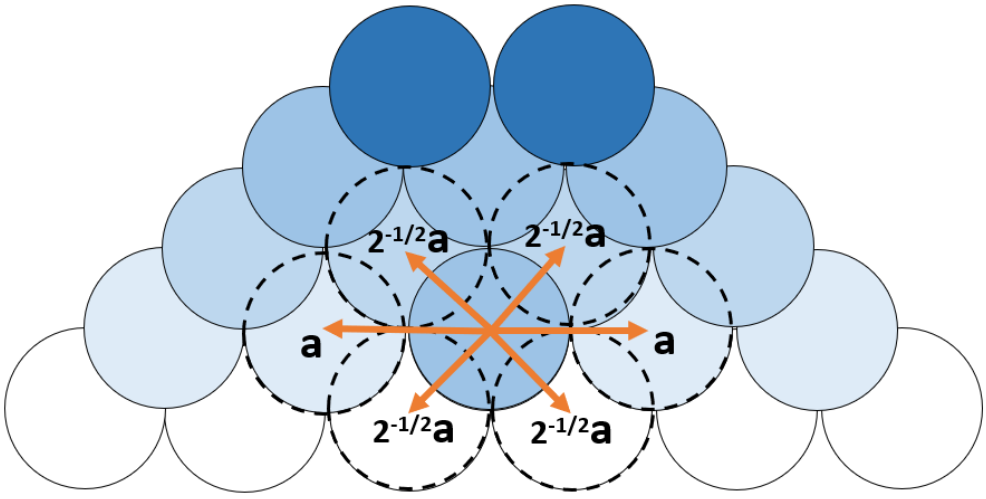

Figure S3. Projection onto a horizontal plane of the distances associated with hopping of an atom on a sloped {111} side facet.

S5. Further details on the refined-MF analysis for $N = N_{cs} + j$ with j = 1-3

For $\boldsymbol{N = N_{cs} + 1}$, the ground state involves a single surface adatom either on the top {100} facet or at the NC base of a closed-shell TP core of size N_{cs} atoms. Thus, the ground state with energy E_N has a degeneracy $\Omega_{GS} = A_{100} + A_{base}$. The first excited state has system energy is $E_N + \phi$. This excited state includes configurations where that adatom is on a {111} side facet with degeneracy A_{111}. However, the first excited state also includes configurations where an atom is removed from the core (specifically from one of the 4 corners of the top {100} facet) and combines with the above-mentioned adatom on the {100} facet or at the NC base to form a dimer. The degeneracy of these configurations is roughly $4(2A_{100} + A_{base})$, the factor of 2 multiplying A_{100} reflecting the 2 dimer orientations on the {100} facets. Of course, there are also higher excited states. Thus, the canonical partition function for the NC of N atoms can be written in the form

$$Q_N = (A_{100} + A_{base}) \exp[-\beta E_N] + \{A_{111} + 4(2A_{100} + A_{base})\} \exp[-\beta\{E_N + \phi\}] + \ldots. \quad \text{(s13)}$$

Thus, the probability of an adatom either on the {100} facet or at the base, $P_{100+base}$, and the corresponding densities $n_{100} \approx n_{base}$, satisfy

$$P_{100+base} \approx (A_{100} + A_{base}) \exp[-\beta E_N]/Q_N \approx 1, \text{ and} \quad \text{(s14)}$$

$$n_{100} \approx n_{base} \approx P_{100+base}/(A_{100} + A_{base}) \approx 1/(A_{100} + A_{base}), \quad \text{(s15)}$$

as noted in the manuscript. On the other hand, the probability, P_{111}, to find at adatom on the {111} facet, and the corresponding density, n_{111}, satisfy

$$P_{111} \approx A_{111} \exp[-\beta(E_N + \phi)]/Q_N, \text{ and} \quad \text{(s16)}$$

$$n_{111} \approx P_{111}/A_{111} \approx \exp[-\beta\phi]/(A_{100} + A_{base}) = \exp[-\beta\phi]\, n_{base}. \quad \text{(s17)}$$

For $\boldsymbol{N = N_{cs} + 2}$, the ground state NC configuration consists of a dimer adsorbed on the {100} top facet (for $N_{cs} \geq 18$), or at the base, of a closed-shell TP "core". As noted in the manuscript, one complication with this case is that when the dimer dissociates, it creates two mobile surface adatoms. As a result, some refinement of the analysis leading to (10) is required. To aid this analysis, **Figure S4** provides a schematic summary of not just the ground state NC configurations, but also of the most relevant low-lying energetically excited states.

Let Ω_{GS} denote the degeneracy of the ground state (GS), and E_{GS} its energy. This corresponds to the number of dimer configurations on the $TP_{mxn,k}$ core core, and is given by

$$\Omega_{GS} = 2(m+n-2) + [(n-k-1)(m-k)+(m-k-1)(n-k)], \quad \text{(s18)}$$

the first term corresponding to dimers at the base, and the last two to dimers on the top {100} facet. Let $\Omega_{ex}(j)$ denote the degeneracy of excited state configuration j in **Figure S4**, then the canonical partition function for the system has the form

$$Q_N = \Omega_{GS} \exp[-\beta E_{GS}] + \sum_{j=1-3} \Omega_{ex}(j) \exp[-\beta\{E_{GS} + \phi)] + \sum_{j=4,5} \Omega_{ex}(j) \exp[-\beta\{E_{GS} + 2\phi)] + \ldots.$$

$$\approx \Omega_{GS} \exp[-\beta E_{GS}]. \qquad \text{(s19)}$$

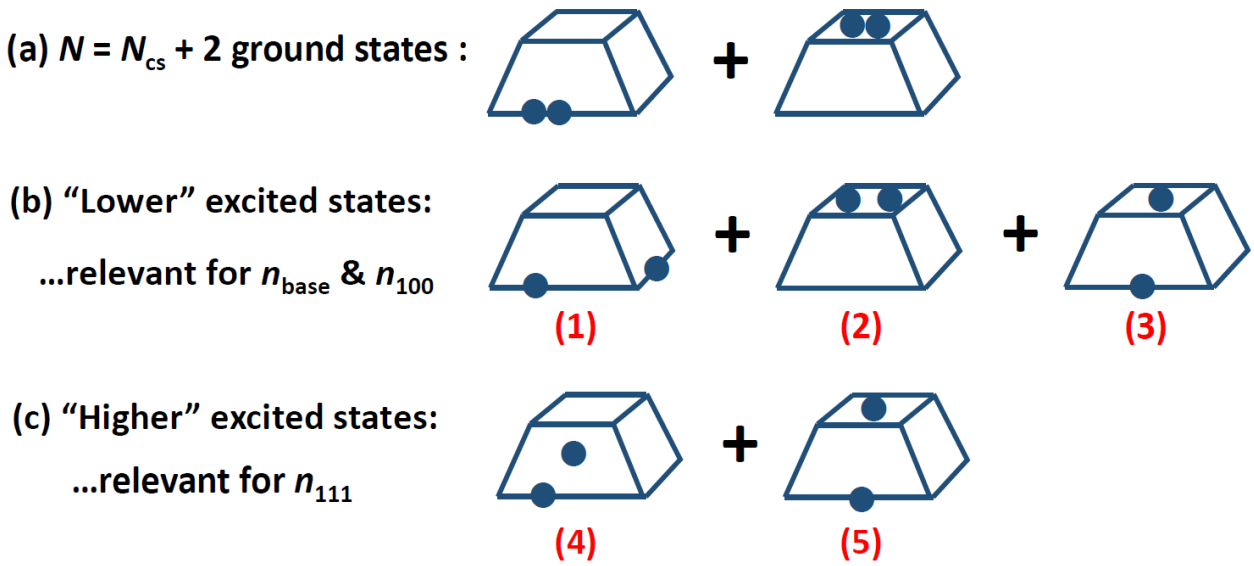

Figure S4. Schematic of ground state and selected low-lying excited state NC configurations for $N = N_{cs} + 2$.

Ignoring more highly excited states, it follows that the density, n_{top}, of mobile surface atoms on the top facet satisfies

$$n_{100} \approx [2\Omega_{ex}(2)/\Omega_{GS} + \Omega_{ex}(3)/\Omega_{GS}] \exp[-\beta\phi]/A_{100} \approx (A_{100} + A_{base} - 1) \exp[-\beta\phi]/\Omega_{GS}, \qquad \text{(s20)}$$

using that $\Omega_{ex}(2) \approx A_{100}(A_{100} - 1)/2$ and $\Omega_{ex}(3) \approx A_{100} A_{base}$. A similar analysis for the density, n_{base}, of mobile surface atoms at the base yields

$$n_{base} \approx [2\Omega_{ex}(1)/\Omega_{GS} + \Omega_{ex}(3)/\Omega_{GS}] \exp[-\beta\phi]/A_{base} \approx (A_{100} + A_{base} - 1) \exp[-\beta\phi]/\Omega_{GS}, \qquad \text{(s21)}$$

using that $\Omega_{ex}(1) \approx A_{base}(A_{base} - 1)/2$ and $\Omega_{ex}(3) \approx A_{100} A_{base}$ (so $n_{100} \approx n_{base}$). Similarly, for the density, n_{111}, of mobile surface atoms on the {111} side facets, one obtains

$$n_{100} \approx [\Omega_{ex}(4)/\Omega_{GS} + \Omega_{ex}(5)/\Omega_{GS}] \exp[-2\beta\phi]/A_{111} \approx (A_{100} + A_{base}) \exp[-2\beta\phi]/\Omega_{GS}, \qquad \text{(s22)}$$

using that $\Omega_{ex}(4) \approx A_{base} A_{111}$ and $\Omega_{ex}(5) \approx A_{100} A_{111}$.

For $\boldsymbol{N = N_{cs} + 3}$, the ground state usually consists of a trimer adsorbed on the {100} top facet (for $N_{cs} \geq 18$) or at the base of a closed-shell "core". See **Figure S5**. Then, Ω_N is the number of locations on the core of linear or bent configurations of the trimer on the top {100} facet plus the number of linear or triangular configurations at the base. Ω_{N-1} is the number of locations on the core of a dimer as specified above in discussion of the case $N = N_{cs} + 2$.

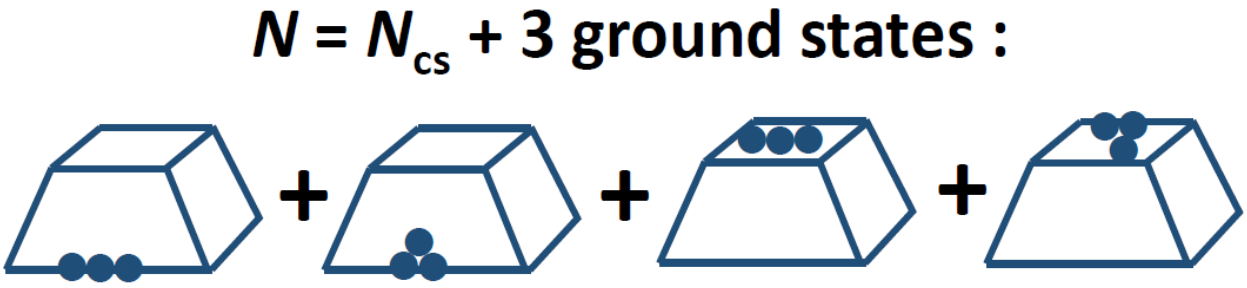

Figure S5. Schematic of ground state NC configurations for $N = N_{cs} + 3$.

S6. Beyond-MF MEP-based treatment of NC diffusion

In Figure 4, we have shown $\delta E(q)$ versus q for N = 50, 51, and 53. For the case of $TP_{5x5,3}$ where N = 50, in **Figure S6** we show the corresponding NC configurations for each q. The 12 atom side facet from which atoms are being removed is shown to the left of the blue arrow. Locations from which those atoms are removed are shown by the red **–** sign. The 12 atom side facet to which a new layer our atoms is being added is shown on the right of the blue arrow. In some cases, there are energetically degenerate configurations which are also shown. For N = 50, $\delta E(q)$ versus q is symmetric about q = 6, and we do not show configurations for q = 7 -12.

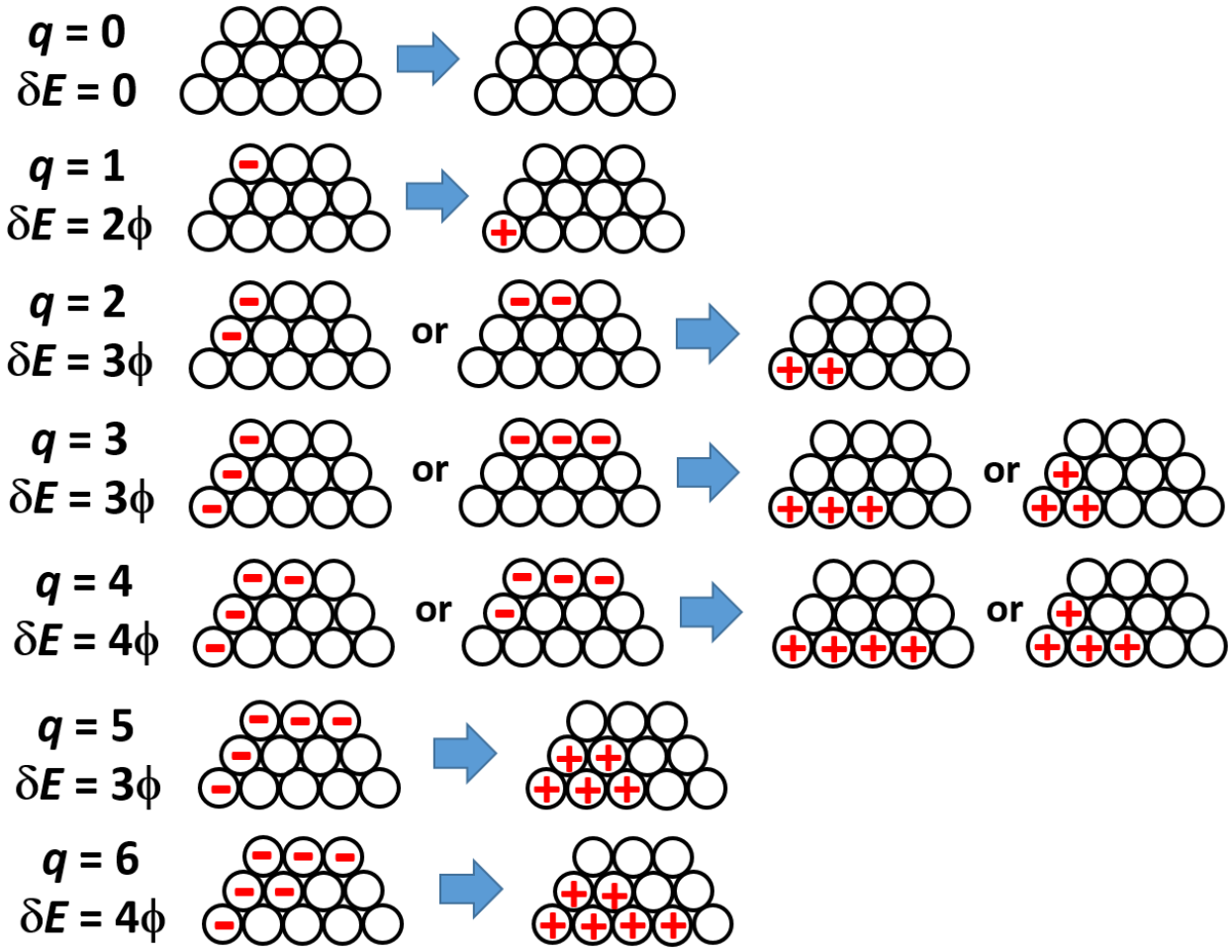

Figure S6. Schematic of configurations on the MEP for a $TP_{5x5,3}$ with N = 50 during disassembly of the outer layer on one facet and formation of a new layer on another facet. Note that these facets have a total of 12 atoms. The **–** shows locations of atoms removed, and the **+** shows the location of atoms added. We also show the energy change $\delta E = \delta E(q)$ for different numbers, q, of transferred atoms.

S7. Master equation based analysis for $N = 52$ versus $N = 53$.

We perform a first-passage time analysis based on the entire MEP profile, $\delta E(q)$ versus q to assess the characteristic time, τ, for disassembly and reformation of outer layers of facets. The diffusion rate for the NC is proportional to $1/\tau$. As noted in Sec. 5.3, with the system starting in state $q = 0$ at time t = 0, let $P(q, t)$ denote the probability to be in state q at time t so that $P(q, 0) = \delta_{q,0}$. Then, one considers the set of master equations

$$d/dt\ P(q, t) = k^+(q-½)P(q-½, t) + k^-(q+½)P(q+½, t) - [k^+(q) + k^-(q)]\ P(q, t), \qquad (s23)$$

where $k^{\pm}(q)$ is the rate to make a transition from state q to state $q \pm ½$ as determined from the energy barriers along the MEP. For $N = 52$ or 53, the total number of atoms transferred is $q_{max} = 12$ then $q = q_{max} = 12$ is assigned as an absorbing or trapping state so that $k^{\pm}(12) = 0$.

Recall that states for integer q correspond to having transferred q atoms from the disassembling facet to the new layer forming on another facet. Higher-energy states for half-integer q correspond to configurations where the adatom being transferred is still on a {111} side facet or hopping around the NC base. The rates, $k^{\pm}(q)$, for $q < 12$ are selected with a Metropolis form satisfying detailed-balance. Specifically, rates for all transitions from states which half-integer q which are downhill in energy have a common value of $k = \nu \exp[-\beta E_{diff}] = k_0$. (Note that **Figure 8** does not explicitly show the presence of an activation barrier, E_{diff}, for a transition from higher-energy states with half-integer q to lower-energy states. Again, E_{diff} is the barrier associated with single-atom diffusion.) For uphill transitions where the state energy increases by $\Delta E > 0$, we set $k = \exp[-\beta \Delta E]\ k_0$. Since $\Delta E = m\ \phi$ for m = 1, 2, or 3, setting $a = \exp[-\beta\phi]$, for uphill transitions one has that $k = a^m\ k_0$. For numerical analysis of the master equations, it is natural to introduce a rescale time variable $x = k_0\ t$, so then rates in the rescaled master equations $d/dx\ P(q,t) = \ldots$ are unity for downhill transitions, and have the form a^m for uphill transitions.

Figure S7 reproduces the MEP for $N = 52$ shown previously in Figure 7, but also indicates the rescaled rates for transitions between adjacent states $q \rightarrow q \pm ½$ (with rates for transitions uphill in energy shown in red font, and rates for downhill transitions in blue font).

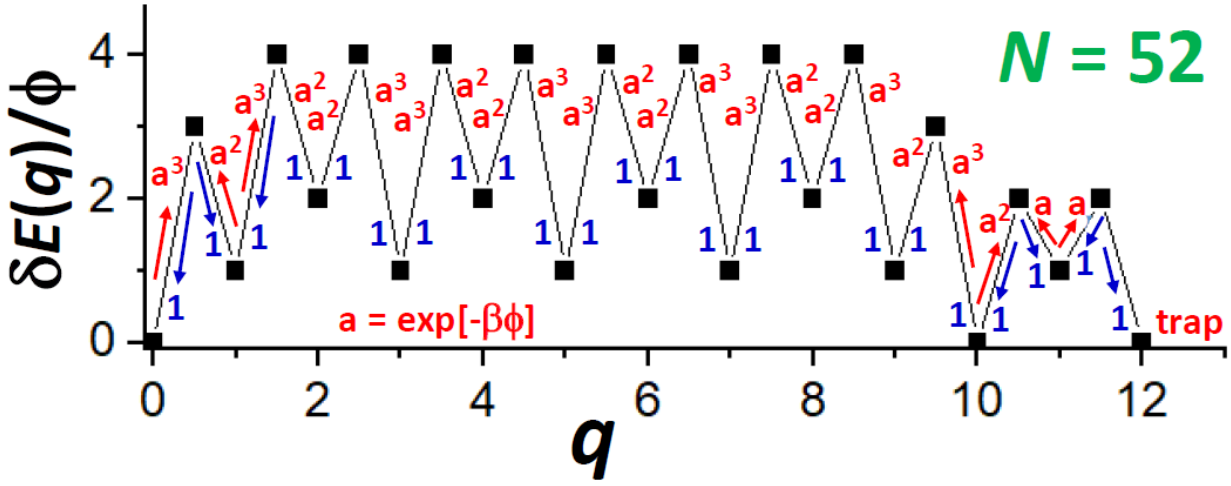

Figure S7. Energies (black square symbols) along the MEP for disassembly and formation of outer layers of NC facets for size N = 52. Also shown are the rescaled rates used in the master equation analysis for transitions between adjacent states along the MEP (typed in red or blue font for each transition).

Using the Mathematica™ type notation $P(q, t)$ = P2q[x = k_0t], for q = 0, ½, 1,…, 12, and P2q′[x] = d/dx P2q[x], the explicit master equations for N = 52 have the form

P0'[x] == P1[x] - P0[x] a^3 ,
P1'[x] == P0[x] a^3 + P2[x] a^2 - 2 P1[x],
P2'[x] == P1[x] + P3[x] - P2[x] (a^2 + a^3),
P3'[x] == P2[x] a^3 + P4[x] a^2 - 2 P3[x],
P4' [x] == P3[x] + P5[x] - 2 P4[x] a^2,
P5'[x] == P4[x] a^2 + P6[x] a ^3 - 2 P5[x],
P6'[x] == P5[x] + P7[x] - 2 P6[x] a^3,
P7'[x] == P6[x] a^3 + P8[x] a^2 - 2 P7[x],
P8'[x] == P7[x] + P9[x] - 2 P8[x] a^2,
P9'[x] == P8[x] a^2 + P10[x] a ^3 - 2 P9[x],
P10'[x] == P9[x] + P11[x] - 2 P10[x] a^3,
P11'[x] == P10[x] a^3 + P12[x] a^2 - 2 P11[x],
P12'[x] == P11[x] + P13[x] - 2 P12[x] a^2,
P13'[x] == P12[x] a^2 + P14[x] a ^3 - 2 P13[x],
P14'[x] == P13[x] + P15[x] - 2 P14[x] a^3,
P15'[x] == P14[x] a^3 + P16[x] a^2 - 2 P15[x],
P16'[x] == P15[x] + P17[x] - 2 P16[x] a^2,
P17'[x] == P16[x] a^2 + P18[x] a ^3 - 2 P17[x],
P18'[x] == P17[x] + P19[x] - P18[x] (a^3 + a^2),
P19'[x] == P18[x] a^2 + P20[x] a^3 - 2 P19[x],
P20'[x] == P19[x] + P21[x] - P20[x] (a^3 + a^2),
P21'[x] == P20[x] a^2 + P22[x] a - 2 P21[x],
P22'[x] == P21[x] + P23[x] - P22[x] 2 a,
P23'[x] == P22[x] a - 2 P23[x],
P24'[x] == P23[x]. (s24)

A similar, but different set of equations were also constructed for the case $N = 53$ based upon the somewhat different MEP shown in Figure 5. With the initial conditions P0[0] = 1 and P2q[0] = 0 for $q > 0$, these equations are integrated until P24[x] increases from 0 to 0.5, i.e., until P24[x_c] = 0.5, and the characteristic time for facet disassembly and formation extracted from $x_c = k_0 \tau$.

Numerical integration of the master equations yields: $x_c = 3.62 \times 10^7$ (1.97×10^7) for $N = 52$ ($N = 53$) when a = 0.02399 (corresponding to $T = 700$ K for Ag NCs); $x_c = 1.50 \times 10^5$ (1.00×10^5) for $N = 52$ ($N = 53$) when a = 0.1 (corresponding to $T = 1130$ K for Ag NCs); and $x_c = 230$ for $N = 52$ and $N = 53$ when a = 1 ($T \rightarrow \infty$).

REFERENCES

[1] P. N. Plessow and C. T. Campbell, *ACS Catal*. 2022, **12**, 2302-2308.
[2] K.C. Lai, Y. Han, P. Spurgeon, W. Huang, P.A. Thiel, D.-J. Liu and J.W. Evans, *Chemical Reviews*, 2019, **119**, 6670-6768 (2019).
[3] K.C. Lai and J.W. Evans, Nanoscale, 2019, **11**, 17506-17516.
[4] C. T. Campbell, S. C. Parker and D. E. Starr, Science 2002, **298**, 811-814.